

# Investigation of Resistive Forces in Variable Recruitment Fluidic Artificial Muscle Bundles

Jeong Yong Kim, Nicholas Mazzoleni, and Matthew Bryant

Department of Mechanical & Aerospace Engineering  
North Carolina State University, Raleigh, NC 27695

## ABSTRACT

This paper experimentally investigates the mechanical behavior of inactive and low-pressure fluidic artificial muscle (FAM) actuators under applied axial load. In most cases, the active characteristics of an actuator are of interest because they provide valuable information about its force-strain relationship. However, a system of actuators requires attention to the interaction between individual units. One such configuration is a bundle of McKibben artificial muscle actuators arranged in parallel and used for load-adaptive variable recruitment. This bio-inspired actuator bundle sequentially increases the number of actuators activated depending on the load required, which is analogous to how motor units are recruited in a mammalian muscle tissue. While using the minimum number of actuators allows the bundle to operate efficiently, the resistive force of inactive elements acts against total bundle contraction due to their inherent stiffness. In addition, when the bundle transitions between recruitment levels, motor units for a given recruitment level may be gradually pressurized; these low-pressure motor units can also cause resistive forces. Experiments were conducted to characterize the complex interaction between the bladder and braided mesh that cause the resistive force and deflection of inactive and low-pressure elements. Based on observations made from experiments, the paper proposes the initial criteria for developing a model of the resistive forces of a McKibben actuator, both individually, and within the context of a variable recruitment bundle.

**Keywords:** McKibben actuator, Fluidic artificial muscle, Variable recruitment, Inactive actuator, Buckling

## INTRODUCTION

In recent years, to address human-robot interface issues in robotic systems, the use of soft actuators has become a topic of great significance. The term “soft actuator” refers to a broad classification of actuators that consist of a compliant component. The inherent compliance of these actuators more closely mimics actuation systems found in nature than traditional rigid robotic linkages and piston-cylinders, which has led to a number of bio-inspired robots that mimic the motion of a caterpillar, snake, and fish, to name a few [1,2,3,4]. In addition, because the compliance of soft actuators is so similar to that of mammalian muscles, many of them have been integrated with human physiology and used for human and animal rehabilitation in the form of soft grippers for a hand and soft ankle-foot orthotics [1,5,6].

One of the limitations of many current soft bio-inspired actuators is that they generate low force outputs in comparison to their rigid counterparts. Fluidic artificial muscles (FAMs), or McKibben actuators, are a class of soft actuator that balances the tradeoffs between force and deflection. These actuators are characterized by a braided mesh helically wound around an elastic tube. When pressurized with fluid (either pressurized air or hydraulic fluid), it expands radially and contracts axially. Its high force-to-weight ratio, inherent compliance, and simple design has made it favorable to robotic applications.

Although McKibben actuators themselves have existed since the 1960s, they have recently received increased attention due to their soft, compliant nature and favorable force capabilities. Applications of McKibben actuators have also become more bio-inspired, as multiple actuators can be combined and actuated in a variable recruitment bundle. A variable recruitment bundle was first introduced by Bryant et al. [7] and consisted of McKibben actuators configured in parallel, as shown in Fig. 1. Just as mammalian muscle consists of motor units that are recruited sequentially based on the required load, in a variable recruitment bundle, individual actuators are divided into motor units, and these motor units are activated in distinct recruitment levels based

on the load requirements of the system. Compared to a single McKibben actuator, the variable recruitment bundle operates at a higher average efficiency and bandwidth [7, 8].

A set of studies has given insight into the design and control of variable recruitment bundles. Jenkins et al. designed variable recruitment controllers and analytically demonstrated efficiency gains and chatter reduction [9], Meller et al. and De La Hunt et al. demonstrated these gains experimentally on both hydraulic and pneumatic artificial muscles, respectively [10, 11]. These studies, while promising, have made a number of simplifying assumptions that make it difficult to capture the complex interactions between individual actuators within a bundle. For example, in variable recruitment, there will be scenarios in which not all actuators are activated simultaneously, allowing active elements to interact with inactive elements. These studies assumed that the resistive force due to these inactive elements was negligible. The purpose of this study is to characterize the forces due to 1) inactive elements at specific recruitment levels and 2) low-pressure elements at partial recruitment levels during recruitment level transitions.

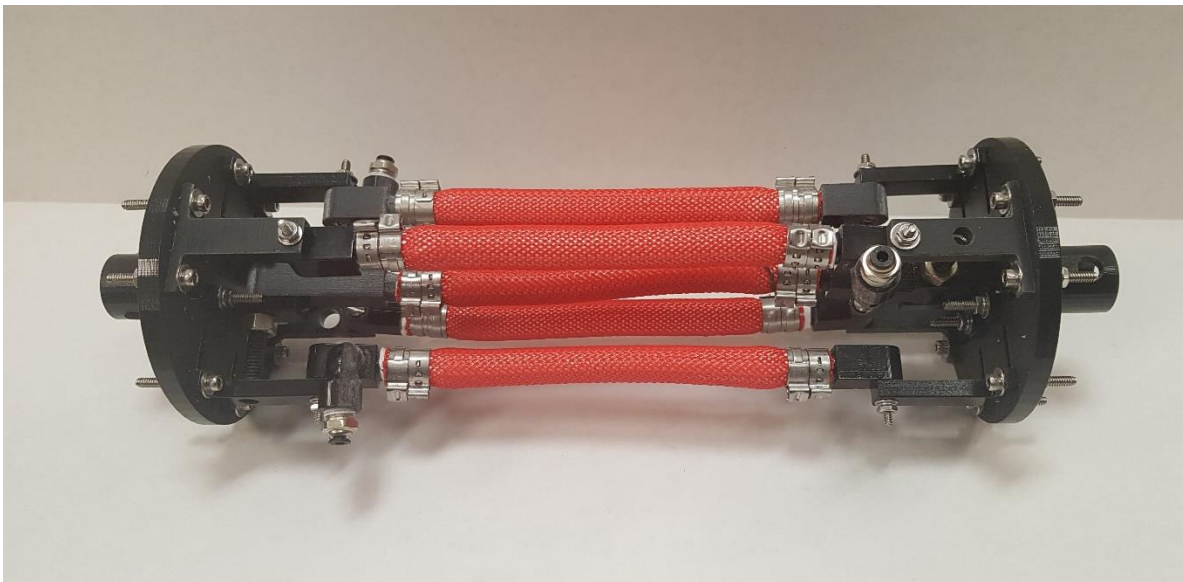


**Fig. 1** One example of a system with multiple soft actuators: a variable recruitment fluidic artificial muscle bundle consisting of multiple McKibben actuators in parallel

### **EFFECT OF INACTIVE ELEMENTS IN A VARIABLE RECRUITMENT BUNDLE**

To observe the effects of inactive elements within a variable recruitment bundle, an experiment was devised to measure the quasi-static force output of a single McKibben actuator from its blocked force condition to its free strain condition. A McKibben actuator with a bladder outer diameter of 12.7 mm, slenderness ratio of 24, and an initial braid angle of 26 degrees was used. A universal material tester (Interactive Instruments Model 1K-16) was used to constrain the actuator at its free length while pressure was applied, thus creating its blocked force condition. A pneumatic pressure supply was used to apply a pressure of 275.8 kPa at the blocked force condition. The testing machine allowed the McKibben actuator to contract sufficiently slowly for the measurement to be assumed as quasi-static until the free strain state was achieved. To compare, another experiment was conducted with the same actuator but with the addition of four inactive actuators centered around and parallel to the active actuator. The inactive actuators are of the same dimension as the active element. The pressure ports of the inactive actuators were open to allow them to vent freely. The actuators were spaced sufficiently to eliminate any effects from the units contacting each other. The result shows that although the blocked force remains the same, as the bundle contracts, the force output was significantly lower than that of a single actuator as shown in Fig. 2. Although the center active unit is producing the same amount of force, the inactive elements apply a force resisting the contraction of the bundle. Consequently, the range of strain during which the bundle outputs positive force decreases. In addition to the reduced force output, a change in slope can be observed which suggests the forces caused by the inactive elements are non-linear.

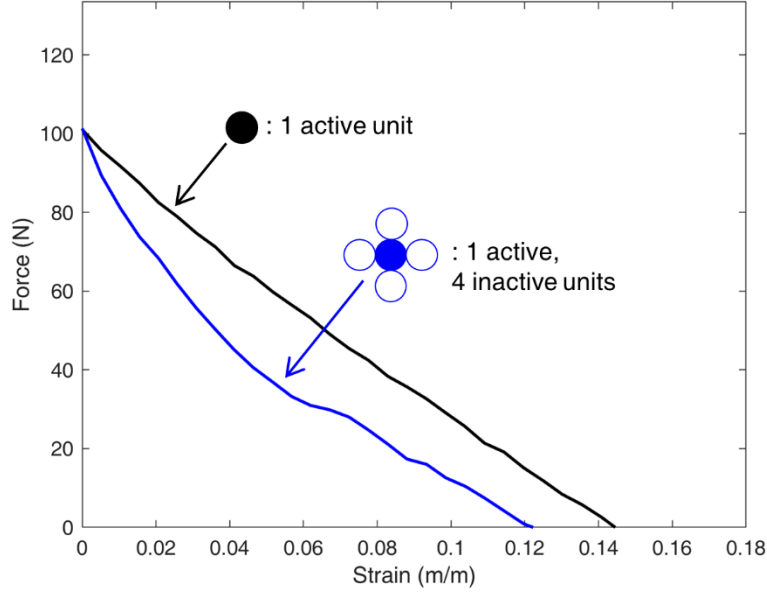


Fig. 2. Quasi-static force output comparison between a single McKibben actuator at 275.8 kPa pressure with and without inactive actuators

### RESISTIVE FORCE PAST FREE STRAIN

The force exerted by inactive elements can be attributed to the elastic forces of the inner bladder. An analytical model was proposed by Ball et al. that expresses the total force output of a McKibben actuator as the sum of the force output due to the kinematic constraints of the braided mesh and the force due to the elastic bladder [12]. The intent of this model was to predict the force-strain behavior of a McKibben actuator up until free strain. The Ball model expresses the total force output of a McKibben actuator unit as:

$$F_{unit} = F_{mesh} + F_{elastic} \quad (1)$$

where  $F_{mesh}$  is the force due to the kinematic constraints of the braided mesh and  $F_{elastic}$  is the force due to the elastic bladder. Fig. 3 illustrates how each force component in Ball's model add up to the total force of a McKibben actuator. The force due to the braided mesh decreases as the unit contracts until the neutral braid angle of  $54.7^\circ$  is reached. This relationship is also dependent on pressure which decides the initial blocked force value. In much of the McKibben actuator literature, this relationship is known as ideal force-strain behavior and is expressed as

$$F_{mesh} = F_{ideal} = (\pi r_0^2) P [a(1 - \varepsilon)^2 - b] \quad (2)$$

$$a = \frac{3}{\tan^2(\alpha_0)}, b = \frac{1}{\sin^2(\alpha_0)} \quad (3)$$

where  $P$  is the applied pressure,  $r_0$  is the initial outer diameter, and  $\alpha_0$  is the initial braid angle [13, 14]. The elastic force due to the bladder starts at zero and is always negative. The sum of the two forces becomes the final output of the McKibben actuator. The force output of a McKibben actuator is associated with the positive portion of the graph, typically characterized by the blocked force and free strain conditions. However, the forces due to inactive elements, as seen in the previous section, are associated with the negative portion of the graph past free strain.

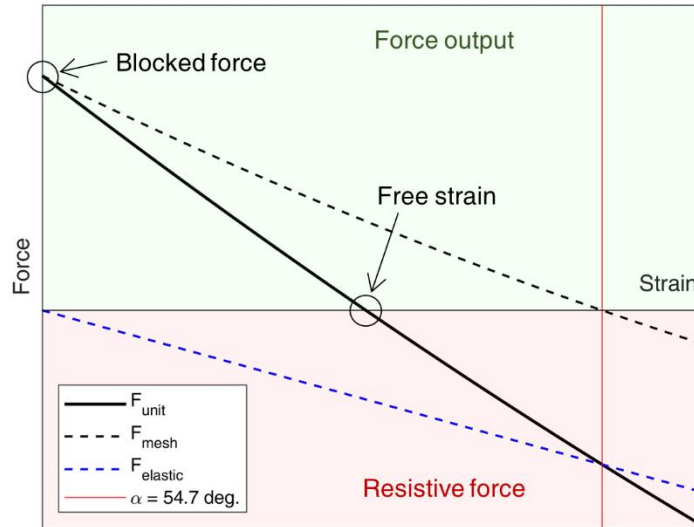


**Fig. 3** Component-wise breakdown of the total force output of a McKibben actuator according to Ball's model

At this point, it is necessary to clearly define the condition for when the total force output of a unit is referred to as *resistive force*. It is possible to refer to the elastic force as resistive force as they are negative components contributing to the total force. However, it is more intuitive to define resistive force according to the direction of the total force of a unit. By doing this, the overall force output of a bundle can be expressed as the difference between mesh forces and elastic forces. The consideration of elastic force as a part of the total force output as proposed by Ball's model provides a base model from which the resistive forces can be understood. The condition for resistive force is defined as:

$$F_{mesh} + F_{elastic} = F_{unit} < 0 \quad (4)$$

According to this definition, resistive forces are not bound to the zero applied pressure condition and manifest whenever the force from the braided mesh is less than the opposing elastic force. The resistive force generated by an inactive unit is a special case in which the applied pressure is equal to zero (i.e., the force generated by the braided mesh is zero). For a pressurized unit, past free strain, the kinematic constraint imposed by the braided mesh produces positive force until the neutral angle is reached, but not enough to overcome the opposing force of the elastic bladder. This has significance in the characterization of the different components of resistive force, as this force cannot be considered separately from the positive output force of a unit but rather as a continuation of the same force as the unit passes through the free strain condition.

### **EXPERIMENTAL OBSERVATION OF RESISTIVE FORCES WITH VARYING PRESSURE**

A typical study on McKibben actuators will measure forces until free strain. However, to understand the overall output force of a variable recruitment bundle, it is necessary to predict the strain at which an actuator unit starts to exert resistive force. For this purpose, a separate set of experiments was conducted measuring the force output of one unit in order to observe the resistive forces. The test setup is the same as the previous experiment, but the stroke of the testing machine was prescribed to intentionally measure the forces past the free strain condition. Additionally, the actuator unit was activated at varying pressures from 34.5 kPa (5 psi) to 103.4 kPa (15 psi) at 34.5 kPa (5 psi) intervals to observe the pressure dependency of resistive force.

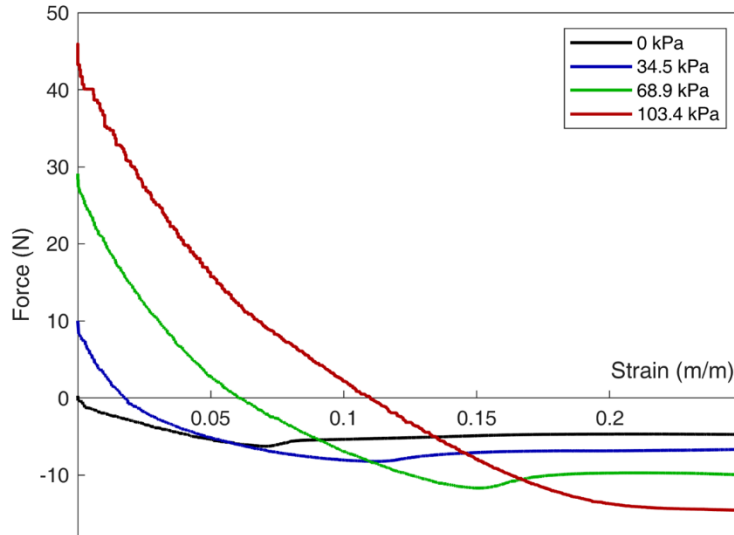


**Fig. 4** The measurement of forces from blocked force to past free strain at varying pressure

The results are shown in Fig. 4. The positive forces show the typical force-strain profiles of McKibben actuators at varying pressure. As defined in the previous section, the resistive forces are the forces measured past free strain. The resistive force when the muscle is inactive is the resistive force at 0 kPa. As observed in the previous experiment, the profiles are non-linear and exhibit a distinct ‘knee’ at which the magnitude of the resistive force reaches a maximum value,  $|F_{resistive}|_{max}$ . Past the strain,  $\epsilon_{min}$  at which this ‘knee’ occurs, the force slightly increases to reach a steady value. It is also noteworthy that the  $|F_{resistive}|_{max}$ ,  $\epsilon_{min}$  and the final value are dependent on the applied pressure. The resistive force is divided into distinct regions based on these observations.

After free strain, the McKibben actuator behaves like a hollow, cylindrical column under axial load. However, the resistive force is the sum of elastic force from the bladder and force transmitted by braided mesh constraint. Therefore, the force from the braided mesh needs to be taken into consideration, as well as the dynamically changing dimensions of the bladder due to pressure. From the experimental observations, this paper proposes a criterion for future model development by dividing the resistive force into three regions as shown in Fig. 5.

- **Region 1** immediately follows the free strain of an actuator unit and extends until wrinkling occurs in the bladder. Wrinkling refers to when the bladder begins to collapse as the cross-sectional area of the bladder starts to deform from its original circular shape. Within this region, the bladder deviates from axisymmetric deformation and starts to buckle, causing transverse deflection. In addition to elastic force, the braided mesh continues to transmit positive force until the braid angle reaches the neutral angle.
- **Region 2** begins as wrinkling occurs in the bladder and extends until its collapse. In this region, the bladder can be considered an inflatable column with thick walls. Collapse occurs as deformation of the bladder cross-section progresses significantly enough that it no longer behaves as a column. If the neutral braid angle has not been reached, the braided mesh continues to exert positive force opposing the force from the bladder. Fig. 6b illustrates the bladder within the mesh as its cross-section deforms from its circular shape.
- **Region 3** follows the collapse of the bladder. The McKibben actuator has deformed significantly in the transverse direction from its linear shape. The bladder has ‘folded’ and behaves analogously to a hinge joint with a torsional spring. Fig. 6c shows a completely collapsed bladder.

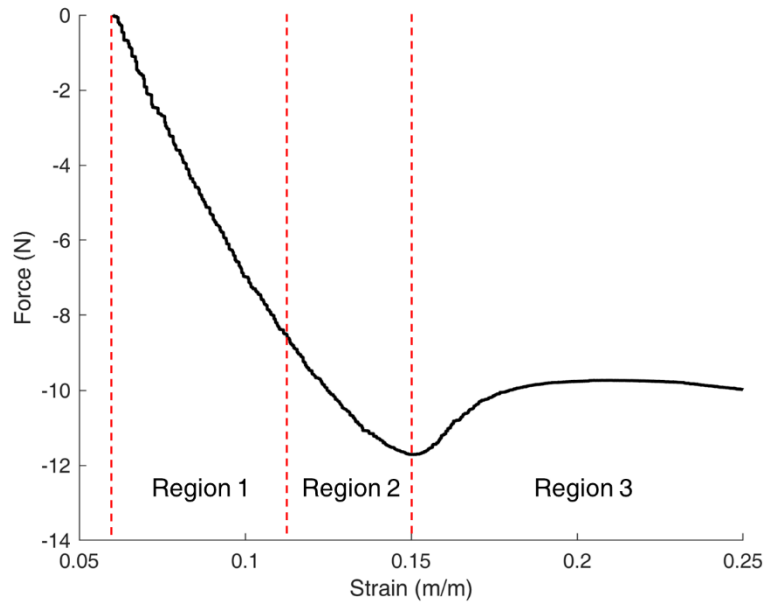


**Fig. 5** Resistive force divided into three regions with boundaries characterized by the wrinkling and collapse internal moment

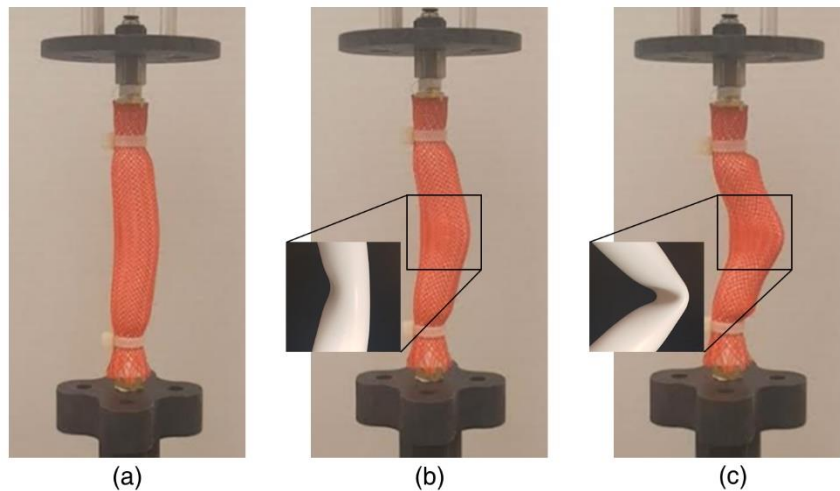


**Fig. 6** Representative pictures of the McKibben actuator at different regions (a) region 1, (b) onset of region 2 as wrinkling occurs, and (c) onset of region 3 as bladder collapses

### **IMPLICATIONS ON OVERALL PERFORMANCE OF A VARIABLE RECRUITMENT BUNDLE**

The ultimate goal of this work is to investigate how the resistive forces generated by inactive and low-pressure elements within a variable recruitment bundle affect overall bundle performance. The effects of inactive elements within a bundle have already been demonstrated in Fig. 2, but this analysis can be extended to investigate the effects of low-pressure elements within a bundle as well. Understanding these effects is important, since in orderly recruitment, the pressure of a given motor unit is slowly increased to system pressure [9]. Current literature does not address the effects that these recruitment transitions have on overall system performance, but understanding these effects may be important, since McKibben actuators with elastic bladders exhibit significant pressure-dependent free strain characteristics, specifically at low pressures. This pressure-dependent free strain is due to the elastic forces in the bladder that act against the force exerted by the mesh. Any force generated by these low-pressure elements past free strain will be negative, and as a result, it is hypothesized that if the actuator is used in a bundle, it will hinder the overall force production.

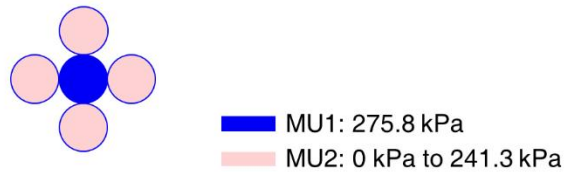


**Fig. 7** Motor Units 1 and 2 and their testing pressure

To validate this hypothesis, an additional experiment was designed. This experiment considered five identical McKibben actuators in a bundle configuration, as shown in Fig. 7. Each actuator had bladder outer diameter of 12.7 mm and slenderness ratio of 24, which were the same dimensions as earlier experiments. The bundle had two distinct motor units (MU1 and MU2), as separate regulators were used to control the pressure of the middle actuator and the outer four actuators. When MU1 is fully active, the bundle is in recruitment level 1 (RL1), and when both MU1 and MU2 are fully active, the bundle is in RL2. When RL2 is not fully active, the bundle is in a partial recruitment level. The pressure of the middle actuator was kept constant at 275.79 kPa (40 psi) and the pressure of the outer four actuators (MU2) could be varied between 0 kPa and 241.32 kPa (35 psi). To establish a baseline, the force-strain behavior of the middle actuator at 275.79 kPa (40 psi) was characterized without the outer four actuators attached. Then, the MU2 actuators were added and force-strain characterizations were performed for MU2 pressures of 0 kPa to 241.32 kPa (35 psi) in increments of 34.5 kPa (5 psi), as the bundle transitioned from RL1 to RL2. These force-strain plots can be seen in Fig. 8. As expected, overall bundle free strain increases from 5 to 35 psi, where it is almost equal to the free strain of the middle actuator at 40 psi. More significantly, there seems to be a range of MU2 pressures during partial recruitment between RL1 and RL2 for which the overall bundle performs better with MU2 completely inactive than with MU2 at low pressures. This phenomenon seems to exist for the 5-15 psi cases, while at 20 psi, the bundle generates more force with an active MU2 than with an inactive MU2. This is visually illustrated in Fig. 9. It is hypothesized that this happens because at lower pressure, the magnitude of the elastic forces exceeds that of the forces generated by the mesh, resulting in resistive forces that decrease overall bundle force. In a bundle with an inactive MU2, there are no pressure-dependent elastic forces that act against the mesh force; there are only axial forces due to the compression of the bladder. Based on the data, these axial compressive forces must be lower in magnitude than the magnitude of the low-pressure elastic forces, a hypothesis is supported by Fig. 4, which shows that at higher strains, resistive forces of low-pressure actuators are greater than those of inactive actuators.

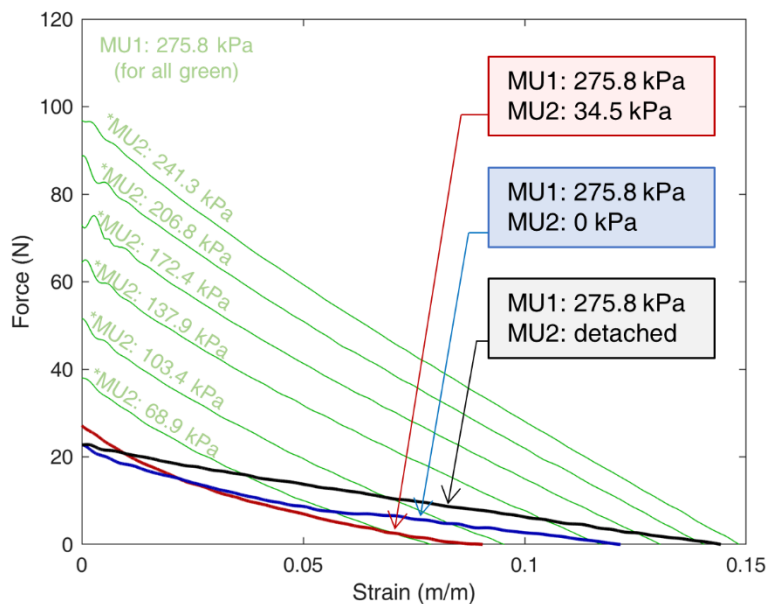


**Fig. 8** Force-strain behavior of a variable recruitment bundle during recruitment level transition

It is important to note that these results do not imply that variable recruitment would be infeasible or would hurt performance; rather, these results show that the contributions of individual actuators in partial recruitment levels is more complex than was previously believed. To address the resistive forces contributed by actuators in partial recruitment levels, it will be necessary to either design controllers that account for these effects or design hardware that prevents actuators from contributing any force to the overall bundle if they are not generating positive force. Using a more inelastic bladder would also help alleviate the elastic contributions at low pressures [15].

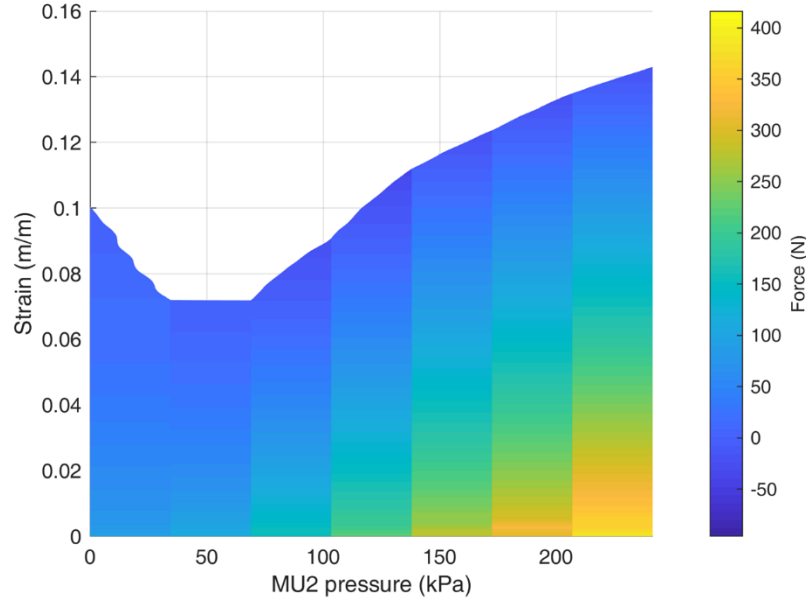


**Fig. 9** Force-strain space at varying MU2 pressures showing a decrease in free strain at low pressures of MU2

Previous literature on variable recruitment bundles have considered the overall force output of a bundle as the sum of the force output of individual elements. When resistive forces are considered, there are some interesting implications especially during transition between recruitment levels. First, let us express the force output of a bundle in the context of Ball's model as

$$F_{bundle} = \sum_{i=1}^N F_{unit,i} = \sum_{i=1}^N (F_{ideal,i} + F_{elastic,i}) \quad (5)$$

Similarly, the same force can be expressed by dividing the units into those contributing positive force and the others acting against the overall force.

$$F_{bundle} = \sum_{j=1}^n F_{output,j} + \sum_{k=1}^{N-n} F_{resistive,k} \quad (6)$$

where  $n$  is the number of units in a bundle exerting a force,  $F_{output}$ , which is the positive force output of those units. In order to calculate the bundle force, it is necessary to accurately calculate the resistive forces generated by each actuator in the bundle past free strain, either by using an analytical formulation (incorporating elastic and compressive force expressions) or by empirically measuring the resistive force generated by each actuator in a bundle as a function of pressure. The latter method would provide a lookup table to calculate exact bundle force as a function of recruitment state, but it would require extensive campaigns of experiments. Future work will involve the use of both of these methods (analytical and empirical) to predict bundle force as a function of recruitment state.

## CONCLUSION

This study experimentally investigated the contribution of the resistive force of inactive and low-pressure actuators to the overall force output of a variable recruitment bundle. It was found that these resistive forces can significantly affect the overall performance of a variable recruitment bundle at partial recruitment levels. An experimental study was carried out to characterize resistive force at varying pressures and some significant trends were identified to guide future attempts to model its behavior. As demonstrated in this paper, the resistive force within a variable recruitment bundle is a component of its overall performance, and an understanding of this resistive force will potentially allow for the optimization of hardware design and control methods for variable recruitment bundles. Although the scope of this study was focused on variable recruitment bundles, this investigation can potentially be extended to any system with multiple soft actuators that exhibit similar resistive behavior.

## ACKNOWLEDGEMENTS

This work was supported primarily by the Faculty Early Career Development Program (CAREER) of the National Science Foundation under NSF Award Number 1845203 and Program Manager Irina Dolinskaya. Additionally, this material is based upon work supported by the National Science Foundation Graduate Research Fellowship Program under Grant No. 1650114. Any Opinions, findings and conclusions or recommendations expressed in this material are those of the author(s) and do not necessarily reflect those of the National Science Foundation.

## REFERENCES

- [1] Rus, D., Tolley, M. T.: Design, fabrication and control of soft robots. *Nature*. 521(7553), 467-475 (2015). doi:<http://dx.doi.org/prox.lib.ncsu.edu/10.1038/nature14543>
- [2] Lin, H., Leisk, G., Trimmer, B. Soft robots in space: a perspective for soft robotics. *Acta Futura* 6, 69–79 (2013)
- [3] Onal, C. D., Rus, D.: Autonomous undulatory serpentine locomotion utilizing body dynamics of a fluidic soft robot. *Bioinspir. Biomim.* 8, 026003 (2013)
- [4] Marchese, A. D., Onal, C. D., Rus, D.: Autonomous soft robotic fish capable of escape maneuvers using fluidic elastomer actuators. *Soft Robotics*. 1, 75–87 (2014)
- [5] Polygerinos, P., Wang, Z., Galloway, K. C., Wood, R. J., Walsh, C. J.: Soft robotic glove for combined assistance and at-home rehabilitation. *Robotics and Autonomous Systems*. 73, 135-143 (2015). <https://doi.org/10.1016/j.robot.2014.08.014>.
- [6] Park, Y., Chen, B.: Design and control of a bio-inspired soft wearable robotic device for ankle-foot rehabilitation. *Bioinspir. Biomim.* 9, 016007 (2014)
- [7] Bryant, M., Meller, M. A., Garcia, E.: Variable recruitment fluidic artificial muscles: modeling and experiments. *Smart Mater. Struct.* 23, 074009 (2014). doi:10.1088/0964-1726/23/7/074009
- [8] Chapman, E. M., Bryant, M.: Bio-inspired passive variable recruitment of fluidic artificial muscles. *Proc. SPIE* 10593, *Bioinspiration, Biomimetics, and Bioreplication VIII*, 105930Y (2018)
- [9] Jenkins, T., Chapman, E. M., Bryant, M.: Bio-inspired online variable recruitment control of fluidic artificial muscles. *Smart Mater. Struct.* 25, 125016 (2016). doi:10.1088/0964-1726/25/12/125016
- [10] Meller, M. A., Chipka, J., Volkov, A., Bryant, M., Garcia, E.: Improving actuation efficiency through variable recruitment hydraulic McKibben muscles: modeling, orderly recruitment control, and experiments. *Bioinspir. Biomim.* 11, 065004 (2016). doi:10.1088/1748-3190/11/6/065004
- [11] De La Hunt, S. A., Pillsbury, T. E., Wereley, N. M.: Variable recruitment in bundles of miniature pneumatic artificial muscles. *Bioinspir. Biomim.* 11, 056014 (2016). doi:10.1088/1748-3190/11/5/056014
- [12] Ball, E., Garcia, E.: Effects of Bladder Geometry in Pneumatic Artificial Muscles. *ASME. J. Med. Devices*. 10(4), 041001 (2016). <https://doi-org.prox.lib.ncsu.edu/10.1115/1.4033325>
- [13] Chou, C., Hannaford, B.: Measurement and modeling of McKibben pneumatic artificial muscles. *IEEE Transactions on Robotics and Automation*. 12(1), 90-103 (1996)
- [14] Tondu, B.: Modelling of the McKibben artificial muscle: A review. *Journal of Intelligent Material Systems and Structures*. 23(3), 225–253 (2012). <https://doi.org/10.1177/1045389X11435435>

[15] Meller, M. A., Bryant, M., Garcia, E.: Reconsidering the McKibben muscle: Energetics, operating fluid, and bladder material. *Journal of Intelligent Material Systems and Structures*. 25(18) 2276-2293 (2014). DOI: 10.1177/1045389X14549872